GENERALIZED CLASSICAL AXIALLY-SYMMETRIC DUAL-REFLECTOR ANTENNAS

Fernando J. S. Moreira* and Aluizio Prata, Jr.
University of Southern California
Los Angeles, CA 90089-0271

A. Introduction

Classical axially-symmetric Cassegrain and Gregorian reflectors are widely used in high-gain antenna applications [1]. The main disadvantage of these configurations is the subreflector blockage, which causes a number of deleterious effects. However, this problem can be reduced by decreasing the main-reflector radiation toward the subreflector. This may be accomplished either by shaping both reflectors [2] or by using alternative classical configurations [3]. This work considers the second option by presenting, in an unified way, generalized classical axially-symmetric configurations that prevent, from a Geometrical Optics (GO) stand point, the main-reflector scattered energy from striking the subreflector surface. Starting from initial design variables, closed-form expressions are derived for the relevant surface parameters, as well as for the corresponding aperture field distributions. These expressions can be used as effective design tools to determine the final antenna geometry, or even to stablish an initial configuration for a shaping procedure.

B. Generalized Classical Axially-Symmetric Configurations

There are four different generalized classical axially-symmetric configurations that avoid the main-reflector scattering toward the subreflector. Their generating curves and relevant parameters are depicted in Figs. 1–4. They are obtained from GO concepts by imposing an uniform-phase field distribution over the antenna aperture (assumed at the plane $z = 0$), starting from a spherical-wave feed source at the antenna focus (located at the coordinate-system origin). The reflector surfaces are yield by spinning the generating curves about the z-axis (symmetry axis). From the figures, D_M and $D_S = 2|X_S|$ are the main- and subreflector diameters, respectively, where X_S is the x-coordinate of the subreflector rim. D_B is the blockage diameter, which sets the x-coordinate of the main-reflector lower point. V_M and V_S are, respectively, the z-coordinates of the main- and subreflector points corresponding to the principal ray. F is the focal length of the parabola generating the main reflector and $2c$ and e are, respectively, the inter-focal distance and eccentricity of the hyperbola or ellipse generating the subreflector. θ_E is the subreflector edge angle and β is the tilt angle between the z-axis and the axis of the subreflector generating conic. The angle θ shown in the figures defines an arbitrary feed-ray direction in the plane $y = 0$. In this work, positive (negative) angular values correspond to counterclockwise (clockwise) angles in the plane shown in Figs. 1–4.

Geometries I (Fig. 1) and II (Fig. 2) have feed-rays with $\theta > 0$ mapped at the aperture region with $x > 0$. However, the subreflector edge ray ($\theta_E > 0$) is mapped at $x = D_M/2$ for Geometry I and $x = D_B/2$ for Geometry II. These two geometries are discussed in Ref. [3]. Geometries III (Fig. 3) and IV (Fig. 4) have feed-rays with $\theta < 0$ mapped at the aperture region with $x > 0$. However, the subreflector edge ray ($\theta_E < 0$) is mapped at $x = D_M/2$ for Geometry III and $x = D_B/2$ for Geometry IV.

0-7803-4178-3/97/$10.00 © 1997 IEEE

In all these configurations the main-reflector generating curve is a parabola, while the subreflector generating curve is a hyperbola for Geometries I and IV and an ellipse for Geometries II and III. The feed is located at one of the hyperbola/ellipse foci and the parabola focus coincides with the other hyperbola/ellipse focus. The basic parameters of the four antenna configurations are summarized in Table 1.

Geometry	I	II	III	IV
Main Reflector	Parabola	Parabola	Parabola	Parabola
Subreflector	Hyperbola	Ellipse	Ellipse	Hyperbola
e	$\|e\| > 1$	$0 < e < 1$	$0 < e < 1$	$\|e\| > 1$
β	$-\pi < \beta < 0$	$0 < \beta < \pi$	$0 < \beta < \pi$	$-\pi < \beta < 0$
θ	$\theta > 0$	$\theta > 0$	$\theta < 0$	$\theta < 0$
θ_E	$\theta_E > 0$	$\theta_E > 0$	$\theta_E < 0$	$\theta_E < 0$
X_S	$X_S > 0$	$X_S > 0$	$X_S < 0$	$X_S < 0$
D_1	D_B	D_M	D_B	D_M
D_2	D_M	D_B	D_M	D_B
θ_1	θ_L	θ_U	θ_L	θ_U
θ_2	θ_U	θ_L	θ_U	θ_L

Table 1: Parameters of the generalized geometries.

In Geometries I and IV the hyperbola can be convex ($e > 1$) or concave ($e < -1$), and $|e| \to \infty$ yields a straight line. In all geometries V_S is a positive quantity and V_M can be either positive or negative. Note that great care should be taken in designing Geometries III and IV to prevent the subreflector reflected rays from intersecting the feed and/or the subreflector surface.

C. Design Equations

For design purposes, the reflectors' generating curves of Figs. 1–4 can be conveniently established from the starting parameters D_M, $D_S = 2|X_S|$, D_B, θ_E, and ℓ_o, where ℓ_o is the total path length from the feed to the antenna aperture (note that $\ell_o/2$ is approximately equal to the distance between the main- and subreflector surfaces). From Figs. 1–4 and the conic-section equations one obtains (for all geometries)

$$\tan\left(\frac{\theta_1}{2}\right) = \frac{D_1}{2\,\ell_o}, \qquad \tan\left(\frac{\theta_2}{2}\right) = \frac{D_2 - 2X_S}{2\,\ell_o - 2X_S\tan(\theta_E/2)}, \tag{1}$$

$$\tan\beta = \frac{\sin\theta_E - \sin\theta_2 + \sin(\theta_E+\theta_2)}{\cos\theta_E + \cos\theta_2 - \sin(\theta_E+\theta_2)/\tan(\theta_1/2)}, \begin{cases}\beta < 0, & \text{Geom. I and IV}\\ \beta > 0, & \text{Geom. II and III}\end{cases} \tag{2}$$

$$V_S = \frac{X_S\sin(\theta_E+\theta_2)\,\sin(\beta+\theta_1)}{\sin\theta_E\,\sin\theta_1\,\sin(\beta+\theta_2)}, \qquad V_M = V_S - \frac{D_1}{2\tan\theta_1}, \tag{3}$$

$$2c = \frac{V_S\sin\theta_1}{\sin(\beta+\theta_1)}, \qquad e = \frac{\sin\theta_1}{\sin\beta + \sin(\beta+\theta_1)}, \qquad F = \frac{D_1 - 4c\sin\beta}{4\,\tan(\theta_1/2)}, \tag{4}$$

where D_1, D_2, θ_1, and θ_2 are defined in Table 1. The commonly encountered classical Cassegrain and Gregorian configurations can be derived from Geometries I and III, respectively, by taking the limit $D_B \to 0$ in Eqs. 1–4 to obtain

$$\theta_L = \beta = 0\,, \qquad \tan\left(\frac{\theta_U}{2}\right) = \frac{D_M - 2X_S}{2\ell_o - 2X_S\tan(\theta_E/2)}\,, \tag{5}$$

$$V_S = \frac{X_S}{2}\left[\cot(\theta_E/2) - \tan(\theta_U/2)\right]\,, \qquad V_M = V_S - \frac{\ell_o}{2}\,, \tag{6}$$

$$2c = \frac{2V_S\sin(\theta_E+\theta_U)}{\sin\theta_U - \sin\theta_E + \sin(\theta_E+\theta_U)}\,, \quad e = \frac{2c}{2V_S - 2c}\,, \quad F = 2c - V_M\,. \tag{7}$$

D. GO Aperture Field Distribution

For design purposes, most of the relevant radiation characteristics of the above configurations can be obtained from the GO aperture distribution. The GO fields are derived by spinning the generating curves of Figs. 1–4 about the z-axis and noting that the astigmatic tube of rays leaving the subreflector has two principal centers of curvature: one located at the ring caustic defined by the rotated parabola focal point and the other located at the intersection of the reflected ray with the z-axis. Assuming the feed radiation as

$$\vec{E}_f(R_f,\theta_f,\phi_f) = \left[E_\theta(\theta_f,\phi_f)\,\hat{\theta}_f + E_\phi(\theta_f,\phi_f)\,\hat{\phi}_f\right]\frac{\exp(-jkR_f)}{R_f}\,, \tag{8}$$

where $\vec{E}_f$ is the radiated electric field and R_f, θ_f, and ϕ_f are the usual observation point spherical coordinates associated with the feed system, the GO electric-field Cartesian components E_X and E_Y at the plane $z = 0$ (aperture) can be shown to be

$$\begin{bmatrix} E_X(\rho_A,\phi_A) \\ E_Y(\rho_A,\phi_A) \end{bmatrix} = \begin{bmatrix} \cos\phi_A & -\sin\phi_A \\ \sin\phi_A & \cos\phi_A \end{bmatrix} \begin{bmatrix} \cos(\phi_f-\phi_A)\,E_\theta(\theta_f,\phi_f) \\ \cos(\phi_f-\phi_A)\,E_\phi(\theta_f,\phi_f) \end{bmatrix}$$
$$\times\ \exp(-jk\ell_o + \Psi)\left|\frac{\tan(\theta/2)}{4F(e^2-1)}\,\frac{[A_1(1+\cos\theta) - A_2\sin\theta]^3}{[A_3(1+\cos\theta) - A_4\sin\theta]}\right|^{\frac{1}{2}}, \tag{9}$$

where

$$\begin{aligned} A_1 &= 1 - e\cos\beta\,, & A_3 &= (c\,A_1 + e\,F)\sin\beta\,, \\ A_2 &= e\sin\beta\,, & A_4 &= F\,(1 + e\cos\beta) + c\,A_2\sin\beta\,, \end{aligned} \tag{10}$$

ρ_A and ϕ_A are the cylindrical coordinates of the aperture point and Ψ is the Gouy phase shift (equal to 0, $\pi/2$, π, and $\pi/2$ for Geometries I, II, III, and IV, respectively). The values of θ, θ_f, and ϕ_f are given by

$$\tan\left(\frac{\theta}{2}\right) = \frac{e\,(\sin\beta + \Delta\cos\beta) - \Delta}{e\,(\cos\beta - \Delta\sin\beta) + 1}\,, \qquad \Delta = \frac{\rho_A - 2c\sin\beta}{2F}\,, \tag{11}$$

$$\theta_f = |\theta|\,, \qquad \phi_f = \begin{cases} \phi_A & \text{when } \theta > 0 \text{ (Geometries I and II)}\,, \\ \phi_A + \pi & \text{when } \theta < 0 \text{ (Geometries III and IV)}\,. \end{cases} \tag{12}$$

E. Conclusions

This work presented closed-form expressions for the surface parameters and aperture field distributions of all possible classical axially-symmetric dual-reflector antenna configurations, including the ones where a blockage diameter is incorporated to reduce the main-reflector scattered energy that strikes the subreflector surface. These expressions are useful design tools and permit considering classical axially-symmetric configurations in an unified and simple way.

References

[1] P. W. Hannan, "Microwave Antennas Derived from the Cassegrain Telescope," IRE Trans. Antennas Propagat., **AP-9**, No. 2, pp. 140–153, March 1961.

[2] V. Galindo, "Design of Dual-Reflector Antennas with Arbitrary Phase and Amplitude Distributions," IEEE Trans. Antennas Propagat., **AP-12**, No. 4, pp. 403–408, July 1964.

[3] Yu. A. Yerukhimovich, "Analysis of Two-Mirror Antennas of a General Type," Telecomm. and Radio Engineering, Part 2, **27**, No. 11, pp. 97–103, 1972.

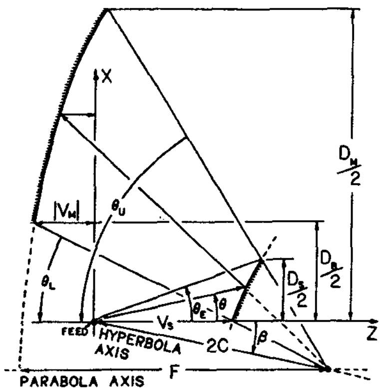

Fig. 1 – Geometry I.

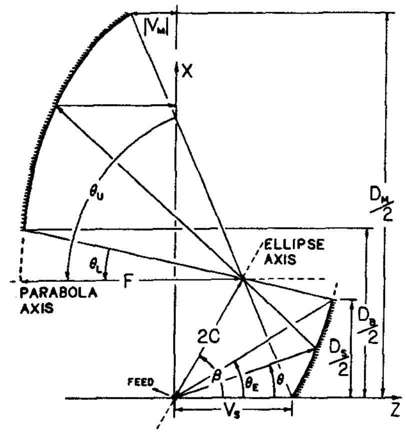

Fig. 2 – Geometry II.

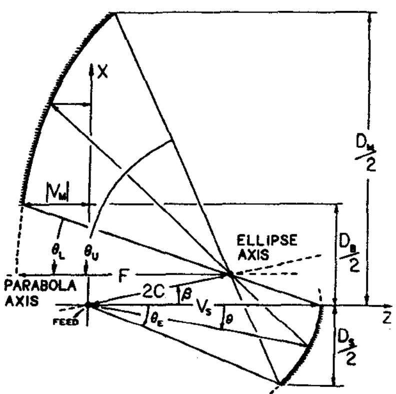

Fig. 3 – Geometry III.

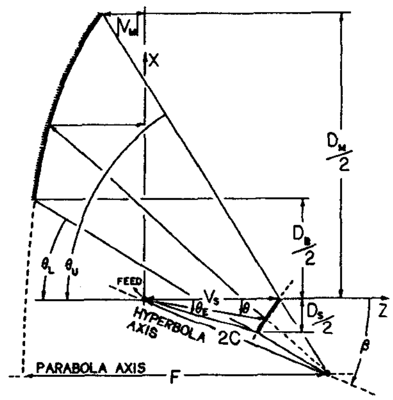

Fig. 4 – Geometry IV.